Dynamics of carrier transport via AlGaN barrier in AlGaN/GaN MIS-HEMTs

C. Ostermaier, P. Lagger, G. Prechtl, A. Grill, T. Grasser, and D. Pogany

Citation: Appl. Phys. Lett. **110**, 173502 (2017); doi: 10.1063/1.4982231
View online: https://doi.org/10.1063/1.4982231
View Table of Contents: http://aip.scitation.org/toc/apl/110/17
Published by the American Institute of Physics

Dynamics of carrier transport via AlGaN barrier in AlGaN/GaN MIS-HEMTs

C. Ostermaier,[1,a] P. Lagger,[1] G. Prechtl,[1] A. Grill,[2] T. Grasser,[2] and D. Pogany[2]
[1]*Infineon Technologies Austria AG, 9500 Villach, Austria*
[2]*TU Wien, 1040 Vienna, Austria*

(Received 15 December 2016; accepted 13 April 2017; published online 24 April 2017)

Exchange of carriers between the GaN channel and the dielectric/AlGaN interface in AlGaN/GaN metal insulator semiconductor high electron mobility transistors was recently attributed to a serial process of electron transport through the AlGaN barrier and electron trapping/emission at the interface. In this paper, the time constant related to barrier transport is evaluated from the measurements of time onset of threshold voltage drift in stress-recovery experiments. Temperature and forward gate bias dependent studies reveal an activation energy of 0.65 eV for the electron transport at zero bias being consistent with the estimated potential barrier of 0.75 eV at the dielectric/AlGaN interface. Thermo-ionic emission and defect assisted tunneling to near interface states are considered as transport mechanisms. *Published by AIP Publishing.*
[http://dx.doi.org/10.1063/1.4982231]

Positive bias temperature instability (PBTI) seen as threshold voltage (V_{Th}) drift after forward gate bias stress is one of the key issues in AlGaN/GaN metal insulator semiconductor high electron mobility transistor (MIS-HEMT) devices, limiting their use for normally off operation regardless of the MIS gate concept. Studies have shown a broad distribution of capture and emission time constants independent of the dielectric material[1–4] and their field- and temperature-dependent acceleration.[5] It appears that the interface state density can be even larger than that one can detect by electrical measurements.[6] Much effort in the preparation of the III-N dielectric interface is needed not only to make these devices applicable in forward-gate-bias operation but also for the optimization and quality of the III-N/dielectric interface which are important for any lateral GaN-based HEMT where such an interface is intrinsically present, e.g., in the passivation layers.

The interface between the III-N layers and the dielectric in a MIS-HEMT is very complex. Electron capture from the GaN channel at the AlGaN/dielectric interface requires electron transport, e.g., trap-assisted hopping and conduction band transport, via the AlGaN barrier. The capture process is thus a serial process, with an effective capture time constant $\tau_{capt,eff}$ being the sum of the capture time constant of the actual defect $\tau_{cap,def}$ and the time constant related to the electron transport in the AlGaN barrier τ_{bar}[1]

$$\tau_{capt,eff} = \tau_{cap,def} + \tau_{bar}. \quad (1)$$

Such a barrier time constant is essentially inversely proportional to the leakage current over the barrier. The experiments in Ref. 1 have indicated a deviation of stress curves at the onset of the ΔV_{Th} increase, which was attributed to the barrier transport effect, but the effect was not so pronounced compared to this result. Furthermore, the role of barrier transport in GaN MIS-HEMTs has been generalized to be included also in the emission processes.[7]

In this work, we utilize pulsed stress-recovery measurements on SiN/AlGaN/GaN MIS-HEMT structures to investigate the role of barrier transport in electron trapping behavior at the III-N/dielectric interface. In comparison to previous results,[1] we use devices with a pronounced onset time for ΔV_{Th} drift which we attribute directly to τ_{bar}. The gate bias V_G and the temperature of the drift onset are used to determine the transport mechanism over the AlGaN barrier.

Devices were made by a state-of-the-art GaN/Si technology using a 25 nm low-pressure chemical vapor deposited SiN layer as a gate dielectric and a 20 nm $Al_{0.2}Ga_{0.8}N$ barrier layer. The stress-recovery experiments were performed using the setup and stressing the scheme described in Ref. 1. For experiments at different biases, a new pristine device was used for stress at each bias. In experiments at the same bias but different stress times, the same device was used. This was possible since even though the total stress time per device is accumulated, the error in ΔV_{Th} is negligible as the stress time is always increased by a factor 10 from one stress to the other and the drift recovers almost entirely before the next stress.

Fig. 1(a) shows a typical recovery of the threshold voltage drift ΔV_{Th} after a forward gate bias of 1.5 V for different stress times. In Fig. 1(b), the ΔV_{Th} for different stress times at $V_G = 1.5$ V is plotted after 100 μs of recovery. It can be clearly recognized that up to 1 ms of stress time, the ΔV_{Th} is indistinguishable from the zero-drift level of the measurement setup. For stress $t_{stress} > 1$ ms, ΔV_{Th} increases. We defined the time at which the ΔV_{Th} clearly increases above the zero-drift level as "drift onset" and extracted its values from the intersections of the extrapolated drift curves with the x-axis (equal to $\Delta V_{Th} = 0$ V).

Fig. 2 shows representative stress-time dependent drift data for −45 °C, +25 °C, 100 °C, and 150 °C at different gate biases. It can be seen that, similar to previous reports,[5] the apparent temperature acceleration of ΔV_{Th} is quite low. This behavior is obvious, as the temperature accelerates both the capture and emission processes. Thus, additional electron

[a]Author to whom correspondence should be addressed. Electronic mail: clemens.ostermaier@infineon.com

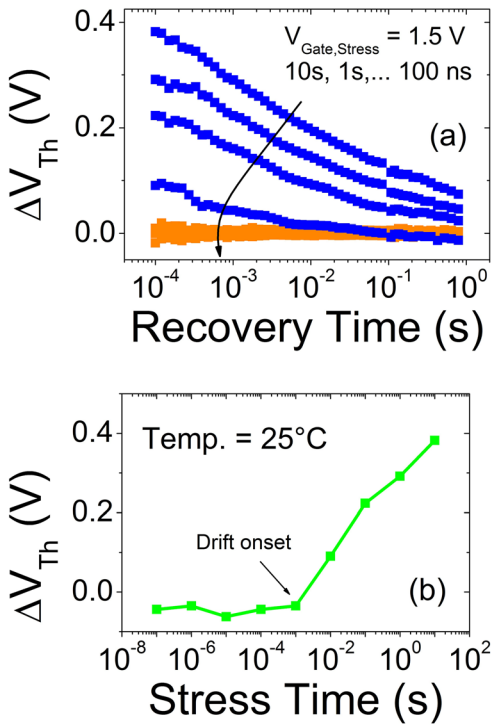

FIG. 1. (a) Recovery plot after different stress times at $V_G = 1.5$ V at 25 °C and (b) corresponding stress plot after 100 μs recovery time showing the drift onset at 1 ms attributed to τ_{bar}. The data in (b) appear in the set of curves in Fig. 2(b) for temperature $\theta = 25$ °C.

captures during gate bias stress are compensated by additional electron emission prior to the initial monitoring time of the measurement setup.[5,8,9] However, the temperature behavior of the drift onset, which we relate directly to τ_{bar}, can still be reliably investigated. We consider that τ_{bar} represents the average time during which the leakage current I_{leak} via the AlGaN barrier produces sufficient free electron charge ($\sim\tau_{bar} * I_{leak}$) at the interface for trapping at the interface states. So, τ_{bar} represents a delay in trapping. The apparent drift onset is only triggered by electron capture, considering that whenever electrons are captured at the interface during stress, the (recovery) emission time constants will be sufficiently broad to recognize the drift within our measurement window (Fig. 1).

Fig. 3 summarizes the temperature- and bias-dependences of the drift onset. In the range of $V_G = 1$–5 V, an *exponential* dependence between the drift onset and stress bias is found, while for $V_G < 1$ V, the drift onset is independent of the stress bias. The Arrhenius plot extracted from data of Fig. 3 is shown in the inset of Fig. 3. The corresponding activation energy E_A of the drift onset τ (Fig. 4) shows a linear dependence on V_G with a plateau around 0.55 eV for $V_G < 1$ V. The linearly extrapolated value of E_A for $V_G = 0$ V is 0.65 eV. For gate biases above 5 V, no effective barrier is seen, indicating that electron capture at the III-N interface solely depends on the defect behavior, i.e., $\tau_{bar} \ll \tau_{cap,def.}$ in (1).

The exponential bias dependence of τ_{bar} on the gate voltage (Fig. 3) suggests that the data could be explained in the framework of the thermo-ionic emission over a potential barrier Φ_{int}

$$\tau_{bar} \approx e^{\frac{\Phi_{int}}{kT}}, \tag{2}$$

where k is the Boltzmann constant, T is the absolute temperature, and Φ_{int} can be expressed as

$$\phi_{Int} = \phi_{Int,0} - V_G \frac{C_{SiN}}{C_{SiN} + C_{Bar}} - \frac{\Delta Q_{Int}}{C_{SiN} + C_{Bar}}, \tag{3}$$

where $\Phi_{Int,0}$ is the interface potential above the Fermi level at equilibrium, i.e., at $V_G = 0$ V (see the inset of Fig. 4).

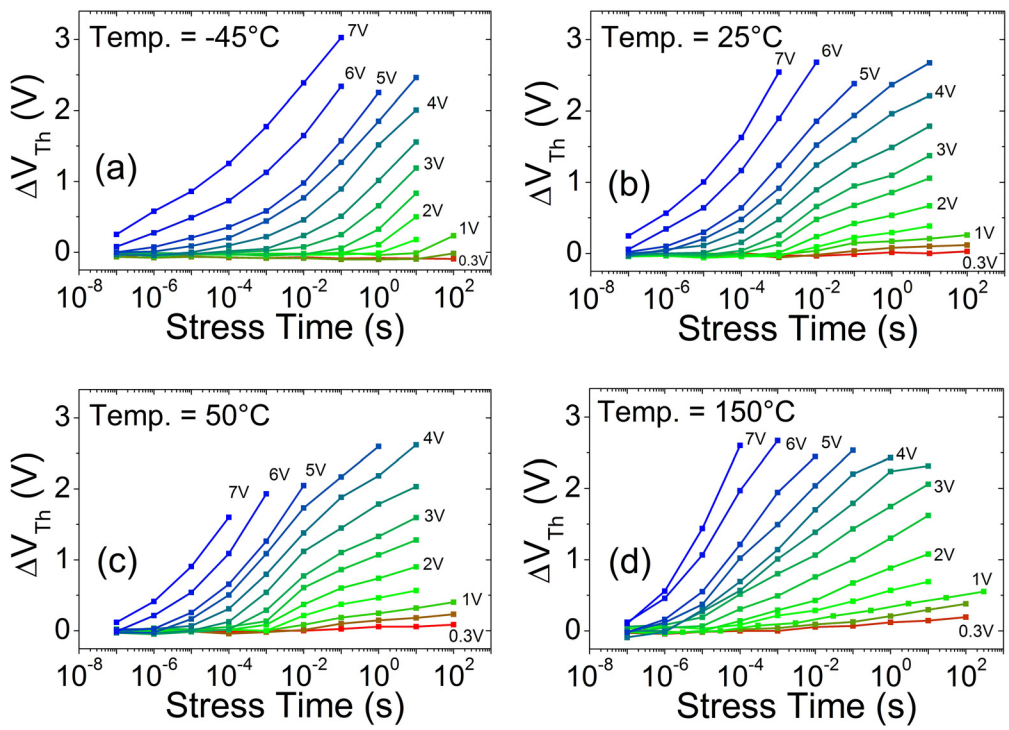

FIG. 2. Selection of stress-time dependent ΔV_{Th} drift data for different gate biases and four different temperatures (a)–(d), extracted 100 μs after the stress.

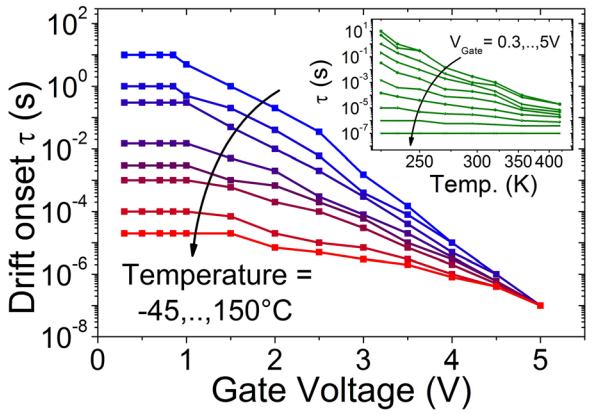

FIG. 3. Summary of the drift onset as a function of V_G for different temperatures −45, −35, −20, 0, 25, 50, 85, and 150 °C. The drift onset was extracted at the intersection of the extrapolated drift curve (Fig. 1(b)) with the x-axis. Times are only plotted down to a minimum stress time of 100 ns resolvable in our setup. The inset shows the corresponding Arrhenius plot for different V_G.

Using the data of Fig. 4, $\Phi_{int,0}$ is equal to 0.65 eV. This value is close to a surface potential of 0.75 eV extracted from device simulation using typical III-N parameters,[10,11] taking into account the 2D-electron density of 7.3×10^{12} cm^{-2} obtained from Hall measurements.

The second term in (3) represents the part of the applied voltage V_G appearing at the interface (i.e., capacitive divider), with C_{SiN} (248 nF/cm^2) and C_{Bar} (421 nF/cm^2) being the area normalized capacitances of the SiN and AlGaN layers, respectively. The last term in (3) represents the potential barrier change due to trapped charge at the interface (ΔQ_{int}). As ΔQ_{int} becomes negative, Φ_{int} increases (i.e., Coulomb effect[5,6]).

Let us discuss now the slope of the activation energy vs. V_G curves at high bias (i.e., $V_G > 1$ V in Fig. 4). According to Eq. (3), this slope is equal to

$$\frac{\partial \phi_{Int}}{\partial V_G} = -\frac{C_{SiN}}{C_{SiN} + C_{Bar}} - \frac{\partial \Delta Q_{Int}/\partial V_G}{C_{SiN} + C_{Bar}}. \quad (4)$$

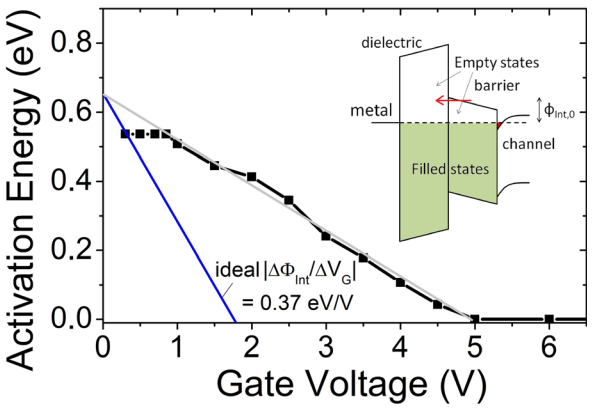

FIG. 4. Extracted apparent activation energy E_A of the drift onset as a function of V_G (symbols). The grey line extrapolates the linear-depending branch of the activation energy towards $V_G = 0$ V. The blue line shows the calculated dependence without considering the effect of charge trapping. Inset: the band diagram of MIS-HEMT at $V_G = 0$ V with indicated parameters. The horizontal red arrow indicates the defect-assisted tunneling mechanism, which is considered to take place at low V_G.

The theoretical value of $C_{SiN}/(C_{SiN} + C_{Bar})$ is 0.37 eV/V, while the experimental absolute value of the slope from Fig. 4 is equal to 0.13 eV/V. This discrepancy indicates that the second term in (4) is non-negligible, meaning that trapping must occur during the stress, even though it is not visible in the experiments. The straightforward explanation is that fast trapping events occur during the stress period, causing ΔQ_{int} to be nonzero (we remark that ΔQ_{int} is negative, which leads to an apparent decrease in the absolute value of the slope). Since the recovery starts before 1 μs after the stress, we assume that the emission event must also be fast, resulting in a negligible ΔV_{Th} shift during measurements. In other words, even if negligible ΔV_{Th} is measured at the drift onset in Fig. 2, the amount of ΔQ_{int} is not negligible. So, in our interpretation, ΔQ_{int} represents a response of traps with emission time constants lower than 1 μs.

The question remains why the second term in (4) is constant, which results in a constant slope of the linear dependence of $\Phi_{int}(V_G)$ observed at large bias in Fig. 4. This can be explained in the framework of the active energy region[11] used to explain the linear increase in ΔV_{Th} with the forward gate bias in MIS-HEMTs.[1] With the increase in V_G, a larger number of interface or border traps in a wider energy region can capture electrons. As this region increases nearly linearly with V_G,[11] the second term in (4) is constant. Comparing the theoretical slope of 0.37 eV/V with the experimental value of 0.13 eV/V and using (4) result in a value of $\partial(\Delta Q_{int})/\partial V_G = -160$ nC/V or an interface concentration of the above mentioned active fast traps of 9.9×10^{11} cm^{-2}/eV. Both values are equivalent interface values, even though these fast traps could also be located within the AlGaN barrier bulk.

The reduced activation energy for $V_G < 1$ V could be explained by a field-enhanced process, e.g., defect-assisted tunneling transport mechanism, allowing an enhanced conductivity through the edge of the barrier near the interface (inset of Fig. 4), similar to what has been suggested for Schottky gate HEMTs.[12,13] The tunneling mechanism, which appears at high electric fields (here appearing at low biases), apparently decreases the thermal activation energy.[14]

It is worth noting that previously reported drift characterization of MIS HEMTs using SiO_2 as a gate dielectric did not indicate such a long drift onset up to milliseconds at room temperature.[1] Thus, we believe that the device reported in this work exhibits a much reduced barrier leakage and an increased effective barrier height, which can be influenced by the temperature and atmosphere during the deposition processes of different dielectric layers.

In conclusions, temperature-dependent drift studies show a rate-limiting time constant which we relate to the electron transport process through the AlGaN barrier in AlGaN/GaN MIS-HEMTs. The activation energy of the electron transport of 0.65 eV at $V_G = 0$ V is comparable to the interface barrier potential, suggesting a predominant transport via the AlGaN conduction band in this structure. For $V_G < 1$ V, a flattening of the activation energy is recognized, indicating a field-enhanced transport mechanism near the III-N/dielectric interface. The slope of the bias dependence of the thermal activation energy indicates that fast traps with time constants much shorter than the measurement setup response of 1 μs, and thus not detectable as drift in the device, are involved in the

modulation of the barrier height for the transport via Coulomb effects. Assuming the validity of the thermo-ionic model, our approach can be thought as a method to monitor the interface potential barrier Φ_{Int} during gate bias stress. Finally, in addition to admittance spectroscopy,[7] our experimental approach represents yet another way to determine barrier properties in fully processed MIS HEMTs without the necessity to study the AlGaN barrier separately, e.g., using Schottky diodes.

[1]P. Lagger, M. Reiner, D. Pogany, and C. Ostermaier, IEEE Trans. Electron Devices **61**, 1022 (2014).
[2]K. Zhang, M. Wu, X. Lei, W. Chen, X. Zheng, X. Ma, and Y. Hao, Semicond. Sci. Technol. **29**(7), 075019 (2014).
[3]Y. Cai, Y. Zhou, K. J. Chen, and K. M. Lau, IEEE Electron Device Lett. **26**, 435 (2005).
[4]S. Liu, S. Yang, Z. Tang, Q. Jiang, C. Liu, M. Wang, and K. J. Chen, in *International Symposium on Power Semiconductor Devices and ICs* (2014), p. 362.
[5]P. Lagger, S. Donsa, P. Spreitzer, G. Pobegen, M. Reiner, H. Haharashi, J. Mohamed, H. Mösslacher, G. Prechtl, D. Pogany, and C. Ostermaier, in *International Reliability Physics Symposium* (2015), pp. 6C.2.1–6C.2.7.
[6]P. Lagger, P. Steinschifter, M. Reiner, M. Stadtmüller, G. Denifl, A. Naumann, J. Müller, L. Wilde, J. Sundqvist, D. Pogany, and C. Ostermaier, Appl. Phys. Lett. **105**, 033512 (2014).
[7]M. Capriotti, P. Lagger, C. Fleury, M. Oposich, O. Bethge, C. Ostermaier, G. Strasser, and D. Pogany, J. Appl. Phys. **117**(2), 024506 (2015).
[8]G. Pobegen, M. Nelhiebel, S. De Filippis, and T. Grasser, IEEE Trans. Device Mater. Reliab. **14**, 169 (2014).
[9]O. Ambacher, B. Fouth, J. Smart, J. R. Shealy, N. G. Weimann, K. Chu, M. Murphy, A. J. Sierakowski, W. J. Schaff, L. F. Eastman, R. Dimitrov, A. Mitchell, and M. Stutzmann, J. Appl. Phys. **87**, 334 (2000).
[10]F. Bernardini, V. Fiorentini, and D. Vanderbilt, Phys. Rev. B **56**, R10024 (1997).
[11]T. Grasser, Microelecton. Reliab. **52**(1), 39–70 (2012).
[12]E. J. Miller, E. T. Yu, P. Waltereit, and J. S. Speck, Appl. Phys. Lett. **84**, 535 (2004).
[13]P. Marko, M. Meneghini, S. Bychikhin, D. Marcon, G. Meneghesso, E. Zanoni, and D. Pogany, Microelecton. Reliab. **52**, 2194 (2012).
[14]G. Vincent, A. Chantre, and D. Bois, J. Appl. Phys. **50**, 5484 (1979).